



**Queensland University of Technology**  
Brisbane Australia

This may be the author's version of a work that was submitted/accepted for publication in the following source:

Jayasundara, Nirmani, Thambiratnam, David, Chan, Tommy, & Nguyen, Andy  
(2019)  
Vibration-based dual-criteria approach for damage detection in arch bridges.  
*Structural Health Monitoring*, 18(5-6), pp. 2004-2019.

This file was downloaded from: <https://eprints.qut.edu.au/203023/>

#### © The Author(s)

This work is covered by copyright. Unless the document is being made available under a Creative Commons Licence, you must assume that re-use is limited to personal use and that permission from the copyright owner must be obtained for all other uses. If the document is available under a Creative Commons License (or other specified license) then refer to the Licence for details of permitted re-use. It is a condition of access that users recognise and abide by the legal requirements associated with these rights. If you believe that this work infringes copyright please provide details by email to [qut.copyright@qut.edu.au](mailto:qut.copyright@qut.edu.au)

**License:** Creative Commons: Attribution-Noncommercial 4.0

**Notice:** *Please note that this document may not be the Version of Record (i.e. published version) of the work. Author manuscript versions (as Submitted for peer review or as Accepted for publication after peer review) can be identified by an absence of publisher branding and/or typeset appearance. If there is any doubt, please refer to the published source.*

<https://doi.org/10.1177/1475921718810011>

# Vibration based Dual Criteria Approach for Damage Detection in Arch Bridges

N. Jayasundara<sup>1</sup>, D.P. Thambiratnam<sup>2</sup>, T.H.T. Chan<sup>2</sup>, A. Nguyen<sup>3</sup>

<sup>1</sup> Queensland University of Technology – Australia, Email: [walpola.jayasundara@hdr.qut.edu.au](mailto:walpola.jayasundara@hdr.qut.edu.au)

<sup>2</sup> Queensland University of Technology – Australia, <sup>3</sup>University of Southern Queensland - Australia

## Abstract

Vibration characteristics of a structure can be used as an indication of its state of structural health as they vary if the structural health is affected by damage. This is the broad principle used in structural health monitoring for vibration based damage detection of structures. Though most structures are built to have a long life span, they can incur damage due to many reasons. Early damage detection and appropriate retrofitting will enable the continued safe and efficient functioning of structures. This study develops and applies a dual criteria method based on vibration characteristics to detect and locate damage in arch bridges. Steel arch bridges are one of the most aesthetically pleasing bridge types, which are reasonably popular in Australia and elsewhere. They exhibit three dimensional and somewhat complex vibration characteristics that may not be suitable for traditional vibration based damage detection methods. There have been relatively fewer studies on damage detection in these bridge types, and in particular the arch rib and struts which are important structural components, have received little attention for damage detection. This study will address this research gap and treat the damage detection in the arch bridge structural components using the dual criteria method to give unambiguous results. The proposed method is first validated by experimental data obtained from testing of a laboratory arch bridge model. The experimental results are also used to validate the modelling techniques and this is followed by damage detection studies on this bridge model as well as on a full scale long span arch bridge. Results demonstrate that the proposed dual criteria method based on the two damage indices can detect and locate damage in the arch rib and vertical columns of deck type arch bridges with considerable accuracy under a range of damage scenarios using only a few of the early modes of vibration.

## Keywords

Structural Health Monitoring, Arch bridge; Vibration based damage detection; Modified modal flexibility method; Modified modal strain energy method; Noise

## Introduction

Bridges are essential components of a road and transport network and are indispensable for the smooth functioning of a city and its economic wellbeing. Most of the bridges in Australia are aging and need to be monitored to ensure that they are capable of accommodating the current transportation needs with increased loads and faster speeds of vehicles. In this context, Structural Health Monitoring (SHM) has recently emerged as a

viable technology to enable the safe operation of both existing and newly built bridges and other structures and the recent Australian Bridge design Code, AS5100<sup>1</sup> refers to the need for SHM in bridges. Vibration characteristics of a structure vary if it incurs damage and this is the principle of vibration based damage detection, one of the key aspects of SHM. It is defined by Chan et al.<sup>2</sup> as the use of an on-structure sensing system to monitor the structural performance and to evaluate the symptoms of anomalies, deterioration or damages that may affect the operation, serviceability, or safety and reliability of a structure. Though structures, especially bridge structures, are designed to have long life spans, they can incur damage due to structural deterioration, environmental effects and random actions such as impacts. Therefore damage detection prior to unexpected incidents or costly repairs has attracted much attention over the years. There has been considerable research on damage detection in simple and complex structures which include beams<sup>3,4</sup>, plate elements<sup>5,6</sup>, trusses<sup>7-9</sup>, offshore platforms<sup>10,11</sup>, bridges<sup>12-15</sup> and rail-track structures<sup>16</sup>.

Precise damage detection is one of the key elements of structural health monitoring. Two basic types of damage detection can be identified as Local methods and Global methods<sup>17</sup>. Non-destructive tests such as ultrasonic, eddy current, acoustic emission, radiography and magnetic particle inspection are local damage detection techniques which require prior knowledge of the damaged region<sup>12</sup>. The limitations of local damage detection techniques were addressed in global methods which examine the changes in vibration properties between the healthy and damaged states of the structure to evaluate the damage. These methods are known as Vibration based Damage Detection Techniques (VBDDTs). Comprehensive literature on VBDDTs provides evidence of the broad research carried out in this field over the past few decades. Damage indices (DIs) based on vibration characteristics are relatively easy to calculate, quick and straightforward and have been widely used to detect, locate and quantify the damages in many structures or structural components<sup>18</sup>.

Arch bridges are aesthetically pleasing structures that have been used across the world, including Australia. Out of the many studies available in the literature on the damage detection of bridges, there are far less on the damage detection of arch bridges compared to other types of bridges. The bridge deck in an arch bridge has received some attention in previous vibration based damage detection (VBDD) studies compared to the more critical load bearing members such as the arch rib, hangers and struts (columns) of arch bridges. The bridge deck is however the most visible component in the bridge and deck damage would be more easily captured by the bridge inspectors than any damage in the other bridge components. From a structural engineering point of view, all the other structural components are equally or more important for the safe operation of the bridge. The failure of one cable/hanger or a strut/column will not be easily visible and can eventually lead to the collapse of at least a part of the bridge and subsequently cause the progressive collapse of the whole bridge. This research will therefore focus on developing and applying reliable

vibration based damage indices that can provide unambiguous results for detecting and locating damage in arch bridge structural components.

The vibration based damage index method recognizes structural damage by considering the changes in the vibration properties between the healthy and damaged states of the structure. Natural frequency has been the parameter used in one of the common approaches as it can be easily measured from just a few accessible points and it is less contaminated by experimental noise <sup>19</sup>. A systematic approach for damage detection using mode shape data was presented by Allemang <sup>20</sup> and Lieven & Ewins <sup>21</sup> using Modal Assurance Criterion (MAC) and Coordinate Modal Assurance Criterion (COMAC) respectively both of which are favourable methods for locating damage.

The Modal Flexibility (MF) method, first proposed by Pandey & Biswas <sup>22,23</sup>, has been used in many damage detection studies due to its accuracy, ease of application and convenient computation <sup>24,25</sup>. Since the structural modal flexibility converges promptly with increasing frequency, few lower natural frequencies and mass normalized mode shape vectors can be advantageously utilized in computing modal flexibilities <sup>22</sup>. This method has been successfully applied in a wide range of structural health monitoring and damage detection cases <sup>26, 27, 23, 5</sup>.

Modal Strain Energy (MSE) method as another VBDDT, was first proposed by Stubbs et al <sup>28</sup>. This method has been then used by many researches utilizing different measured data for different types of structures <sup>9,8</sup>. A multi-criteria approach incorporating MF and MSE methods was proposed by Shih et al. <sup>5</sup> for damage detection in beams and slabs in which they were able to detect single and multi-damages. It was shown that the MSE method is capable of detecting single as well as multiple damages while the MF method is only good for single damage cases. However the application of these methods for damage detection in arch bridges is not evident in the literature. Arch bridges exhibit three dimensional and somewhat complex vibration characteristics which involve the deck, rib and the struts (and as demonstrated later) are not very favourable for traditional vibration based damage detection methods.

This paper develops and applies a dual criteria approach which simultaneously uses damage indices (DIs) based on modified forms of the MF and MSE methods to provide unambiguous results for detecting and locating damage in the main structural components of deck type arch bridges. The superior performance of the proposed method compared to traditional methods is demonstrated through the comparison of the results. Using the 2 DIs simultaneously enables the results obtained from either DI to complement and supplement the results from the other DI and lead to more reliable prediction of the damage location. Prior to its application, the proposed method is validated through experimental testing of an arch bridge model under laboratory conditions with limited number of sensors. The feasibility of the proposed method is demonstrated through its application to a range of damage detection scenarios.

## Method

A dual criteria approach using two different damage indices is developed and applied to detect and locate damage in arch bridges. These indices are modified versions of the traditional damage indices based on the modal flexibility and modal strain energy methods, which are briefly presented below.

### Modal flexibility method

Modal flexibility  $F$  at a location  $j$  of a linear structure can be expressed as [Eq. 1](#);

$$[F] = \sum_{i=1}^m \frac{1}{\omega_i^2} \phi_i \phi_i^T \quad (1)$$

where  $i$  is the mode number considered and  $\omega_i$  and  $m$  are the natural frequency of the structure at mode  $i$  and the total number of modes considered, respectively.  $\phi_i$  is the  $i^{\text{th}}$  mode shape vector and  $\phi_i^T$  is its transpose.

According to Pandey & Biswas<sup>22</sup> the Modal Flexibility Change ( $MFC$ ) can be expressed as in [Eq. 2](#) where  $d$  and  $h$  denotes the damage and healthy conditions respectively .

$$MFC = [F]_d - [F]_h = \left[ \sum_{i=1}^m \frac{1}{\omega_i^2} \phi_i \phi_i^T \right]_d - \left[ \sum_{i=1}^m \frac{1}{\omega_i^2} \phi_i \phi_i^T \right]_h \quad (2)$$

The diagonal values of MFC matrix are extracted and each term represents the modal flexibility at a particular location along the member.

Modal Flexibility Damage Index (MFDI) is obtained by dividing MFC value of a particular location by MF value extracted from  $[F]$  of that same location at healthy state. Therefore the normalized damage index at location  $j$  at  $i^{\text{th}}$  mode can be written as [Eq. 3](#)

$$MFDI_{ij} = \frac{\left[ \sum_{i=1}^m \frac{1}{\omega_i^2} \phi_i \phi_i^T \right]_D - \left[ \sum_{i=1}^m \frac{1}{\omega_i^2} \phi_i \phi_i^T \right]_H}{\left[ \sum_{i=1}^m \frac{1}{\omega_i^2} \phi_i \phi_i^T \right]_H} \quad (3)$$

### Modal strain energy method

MSE based method proposed by Stubbs et al.<sup>28</sup> has been improved to suit the damage detection in arch bridges.

For a general Euler-Bernoulli beam, the  $i^{\text{th}}$  modal strain energy can be given by [Eq. 4](#),

$$U_i = \frac{1}{2} \int_0^L k [\phi_i''(x)]^2 dx \quad (4)$$

where  $k$  is the bending stiffness of the beam ( i.e the product of its Young's modulus  $E$  and the second moment of area  $I$ ) and  $\phi_i(x)$  is the mode shape of  $i^{\text{th}}$  modal vector.

If the beam is sub divided in to N elements, the modal strain energy associated in the  $j^{th}$  element or the contribution of  $j^{th}$  element to the total modal strain energy is  $C_{ij}$ ; which is given by [Eq. 5](#), where  $k_j$  is the bending stiffness of the  $j^{th}$  element, which is equal to  $(EI)_j$

$$C_{ij} = \frac{1}{2} \int_j k_j [\phi_i''(x)]^2 dx \quad (5)$$

For a prismatic member,  $EI$  remains constant and hence  $k_j$  in [Eq 5](#) is equal to  $k$  in [Eq 4](#). The fraction of the modal strain energy for the  $i^{th}$  mode that is concentrated in the  $j^{th}$  element is given by  $F_{ij}$  and  $F_{ij}^*$  in [Eq. 6](#), in its healthy and damaged states respectively. In this equation and in what follows, the modal parameters associated with damaged element are denoted by asterisks.

$$F_{ij} = \frac{C_{ij}}{U_i} \quad \text{and} \quad F_{ij}^* = \frac{C_{ij}^*}{U_i^*} \quad (6)$$

where  $C_{ij}^*$  and  $U_i^*$  are given by

$$C_{ij}^* = \frac{1}{2} \int_j k_j^* [\phi_i''^*(x)]^2 dx \quad \text{and} \quad U_i^* = \frac{1}{2} \int_0^L k^* [\phi_i''^*(x)]^2 dx \quad (7)$$

In the above equations  $k_j^*$  and  $k^*$  denote the flexural stiffness of the damaged element and the damaged beam (member) respectively.

When the beam is sub divided in to large number of elements, the fraction of modal strain energy concentrated in each element is very small; such that for any mode  $i$ , the term  $F_{ij}$  and  $F_{ij}^*$  have the following properties;

$$\sum_{j=1}^N F_{ij} = \sum_{j=1}^N F_{ij}^* = 1; \quad \text{and} \quad F_{ij} \ll 1, F_{ij}^* \ll 1 \quad (8)$$

where  $N$  is the number of elements in a member.

If the damage is assumed to be located at a single subdivision, the fractional strain energy of that element remains relatively constant resulting in

$$F_{ij} \cong F_{ij}^* \quad (9)$$

If the flexural rigidity ( $EI$ ) is essentially constant over the entire length of the member for both the damaged and undamaged modes,  $k$  of  $U_i$  and  $k^*$  of  $U_i^*$  are assumed to be equal <sup>29</sup>. Therefore, the [Eq 9](#) can be rearranged so that the ratio of the stiffness  $k_j^*$  of the damaged element to its stiffness  $k_j$  in the undamaged state is obtained as:

$$\frac{k_j}{k_j^*} = \frac{\int_j [\phi_i''^*(x)]^2 dx / \int_0^L [\phi_i''^*(x)]^2 dx}{\int_j [\phi_i''(x)]^2 dx / \int_0^L [\phi_i''(x)]^2 dx} = \frac{f_{ij}^*}{f_{ij}} \quad (10)$$

To avoid the possible singularity problems with the  $\frac{f_{ij}^*}{f_{ij}}$ , shifting the axis of reference to avoid numerical sensitivities is recommended by Stubbs & Garcia <sup>30</sup>. Therefore  $f_{ij}$  and  $f_{ij}^*$  are now considered as  $1 + f_{ij}$  and  $1 + f_{ij}^*$  respectively.

The damage indicator  $\beta_{ij}$  is given by,

$$\beta_{ij} = \frac{1 + f_{ij}^*}{1 + f_{ij}} \quad (11)$$

Substituting [Eq10](#) in to [Eq11](#) forms,

$$\beta_{ij} = \frac{k_j}{k_j^*} = \frac{\left( \int_j [\phi_i''(x)]^2 dx + \int_0^L [\phi_i''(x)]^2 dx \right) \int_0^L [\phi_i''(x)]^2 dx}{\left( \int_j [\phi_i''(x)]^2 dx + \int_0^L [\phi_i''(x)]^2 dx \right) \int_0^L [\phi_i''(x)]^2 dx} \quad (12)$$

Numerically, it can be expressed as follows:

$$\beta_{ij} = \frac{k_j}{k_j^*} = \frac{\left[ (\phi_i''^*)^2 + \sum (\phi_i''^*)^2 \right] \left[ \sum (\phi_i'')^2 \right]}{\left[ (\phi_i'')^2 + \sum (\phi_i'')^2 \right] \left[ \sum (\phi_i''^*)^2 \right]} \quad (13)$$

### Modified damage indices vs traditional damage indices

Arch bridges exhibit three dimensional and rather complex vibration. But, the initial global modes of vibration of the whole arch bridge are governed by the mode shapes of the arch rib with dominant contributions in the lateral and vertical directions, in which the maximum mass participations occur. Table 1 presents the ratios of effective mass to total mass fractions of the first four modes of Cold Canyon Bridge extracted from its finite element model. It can be seen that modes 1 and 2 in the lateral and mode 3 in the vertical direction are dominant modes with high mass participation.

**Table 1:** Ratios of effective mass fractions of the first four modes of Cold Spring Canyon bridge

Mode Number	Ratios of effective mass to total mass		
	X (lateral)	Y (vertical)	Z
01	<b>0.5117</b>	0.5857E-04	0.3323E-09
02	<b>0.2066</b>	0.1893E-03	0.4094E-08
03	0.1658E-09	<b>0.56455</b>	0.1076E-08
04	<b>0.5040</b>	0.1650E-04	0.1875

Therefore instead of using the resultant mode shapes as in the traditional DI methods, decomposed mode shapes using the lateral and vertical components are used to create the modified DIs used in this study. To facilitate the use of these component specific features, the DIs are modified as follows.

$$MFDI_{ijV} = \frac{\left[ \sum_{i=1}^m \frac{1}{\omega_i^2} \phi_i \phi_i^T \right]_{DV} - \left[ \sum_{i=1}^m \frac{1}{\omega_i^2} \phi_i \phi_i^T \right]_{HV}}{\left[ \sum_{i=1}^m \frac{1}{\omega_i^2} \phi_i \phi_i^T \right]_{HV}} \quad (14)$$

$$MFDI_{ijL} = \frac{\left[ \sum_{i=1}^m \frac{1}{\omega_i^2} \phi_i \phi_i^T \right]_{DL} - \left[ \sum_{i=1}^m \frac{1}{\omega_i^2} \phi_i \phi_i^T \right]_{HL}}{\left[ \sum_{i=1}^m \frac{1}{\omega_i^2} \phi_i \phi_i^T \right]_{HL}} \quad (15)$$

The above expressions define the modified DIs based on MF where the subscripts  $L$  and  $V$  denote the lateral and vertical component specific DIs using and lateral and vertical components of mode shapes respectively.

The modal strain energy based method can be similarly modified and  $\beta_{ijV}$  and  $\beta_{ijL}$  are the vertical and lateral component specific DIs using the lateral and vertical components of mode shapes respectively.

$$\beta_{ijV} = \frac{k_j}{k_j^*} = \frac{\left[ (\phi_{iV}^{**})^2 + \sum (\phi_{iV}^{**})^2 \right] \left[ \sum (\phi_{iV}^{**})^2 \right]}{\left[ (\phi_{iV}^{**})^2 + \sum (\phi_{iV}^{**})^2 \right] \left[ \sum (\phi_{iV}^{**})^2 \right]} \quad (16)$$

$$\beta_{ijL} = \frac{k_j}{k_j^*} = \frac{\left[ (\phi_{iL}^{**})^2 + \sum (\phi_{iL}^{**})^2 \right] \left[ \sum (\phi_{iL}^{**})^2 \right]}{\left[ (\phi_{iL}^{**})^2 + \sum (\phi_{iL}^{**})^2 \right] \left[ \sum (\phi_{iL}^{**})^2 \right]} \quad (17)$$

For both methods a single indicator is generated by taking several global modes into account as follows.

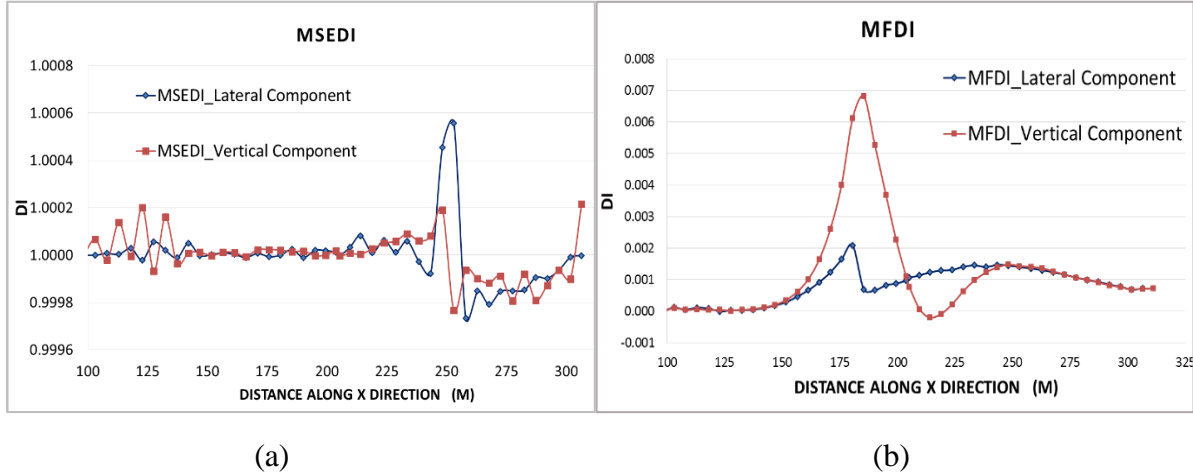
$$\beta_j \text{ or } DI_j = \frac{\sum_{i=1}^{NM} Num_{ji}}{\sum_{i=1}^{NM} Denom_{ji}} \quad (18)$$

In the above Eq,  $NM$  refers to the number of modes and  $Num_{ji}$  and  $Denom_{ji}$  are the numerator and denominator of any one the Eqs (14), (15), (16) or (17), depending on the particular DI.

To illustrate the performance of the component specific DIs based on both MF and MSE, two cases of arch rib damage in the 213m span Cold Spring Canyon Bridge (described later in the section titled Damage detection in full scale two hinged arch bridge) are treated. In Figure 1 (a) results for the (lateral and vertical) component specific DIs based on MSE for rib damage at 250m are compared. It is clearly evident that the lateral component specific DI performs much better than its vertical counterpart. Figure 1(b) compares the results from both component specific damage indices based on MF for damage in the arch rib at 180m. In this case, the vertical component specific DI performs better than its horizontal counterpart.



It is therefore evident that depending on the location of the damage, one of the component specific DI, based on either MSE or MF method, can perform better than the other. The numerical value of this component DI will be higher compared with that of the other component DI as illustrated in Figure 1.



**Figure 1:** Lateral and Vertical (a) MSE and (b) MF DI curves of Cold Spring Canyon Bridge (section 3.2) under two cases of rib damage

To obtain the best possible results, it is hence necessary to select (and use) the component specific DI which performs better than its counterpart, for both MF and MSE based DIs. Towards this end, the above modal flexibility and modal strain energy methods can be further modified as shown in [Eq. 19](#) and [Eq. 20](#).

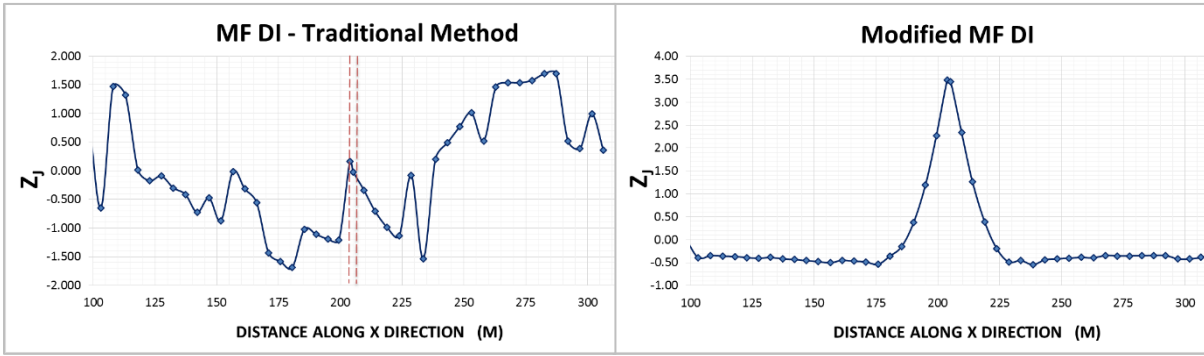
For the MSE case, the better performing DI is selected by comparing the results of  $\beta_{jV}$  and  $\beta_{jH}$ . The same is done with the 2 component specific MFDIs. That is for damage detection at any location the prominent  $\beta_j$  and  $DI$  are obtained by selecting the larger of the two component specific DIs.

$$\beta_j = [\max(|\beta_{jV}|, |\beta_{jH}|)] \quad (19)$$

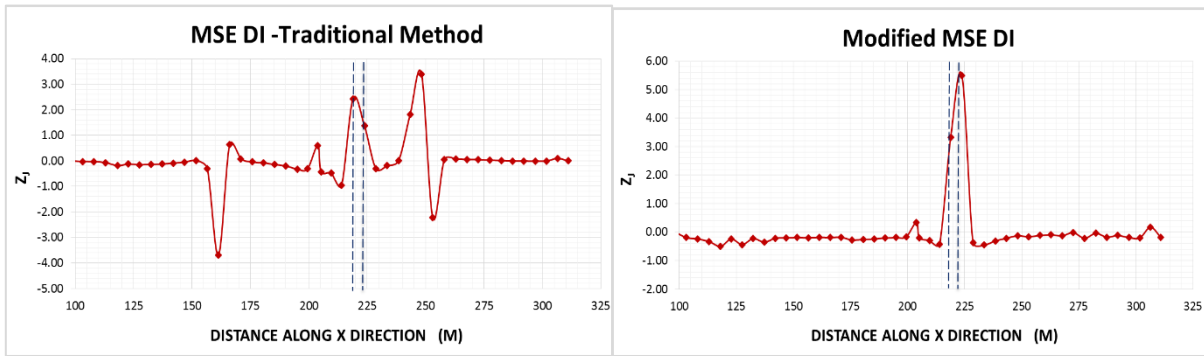
$$DI = [\max(|DI_V|, |DI_H|)] \quad (20)$$

The selected  $\beta_j$  and  $DI$  are then normalized as shown in [Eq. 21](#) below, in which  $\bar{\beta}$  and  $\bar{DI}$  are the mean values and  $\sigma_{\beta}$  and  $\sigma_{DI}$  are standard deviations of  $\beta_j$  and  $DI$  respectively.

$$Z_j = \frac{\beta_j - \bar{\beta}}{\sigma_{\beta}} \text{ or } Z_j = \frac{DI - \bar{DI}}{\sigma_{DI}} \quad (21)$$



(a)



(b)

**Figure 2:** Comparison of (a) Traditional and Modified MF DIs and (b) Traditional and Modified MSE DIs for damage detection in 213m span Cold Canyon Bridge

To illustrate this choice and compare the performance of the selected component specific DIs with those from the traditional DIs, two arch rib damage cases involving damage at 205 m and 220 m in the same Cold Spring Canyon Arch Bridge are considered.

Results in Figure 2 clearly show the superior performance of the selected component specific DIs compared to those of the traditional DIs based on both MSE and MF. The enhanced ability of the proposed method to detect damage compared to the traditional methods is clearly evident as there is less ambiguity, no false alarms and there is a more definite indication of the damage location. Though results from either one of the selected component specific DI based on either MF or MSE would give unambiguous results, as seen in Figure 2, this study recommends that results from both DIs be used as they can complement and supplement each other and provide adequate confidence in the predictions.

The method proposed in this paper therefore has three parts:

1. Use the modal data to calculate the 4 component specific (or modified) DIs based on MF and MSE
2. Use the above selection criteria (Eq.19- 21) to determine the better performing modified DIs of both types (ie based on MF and MSE)
3. Plot the results from both selected modified DIs to obtain unambiguous predictions

The entire procedure can be automated to make it easier to use.

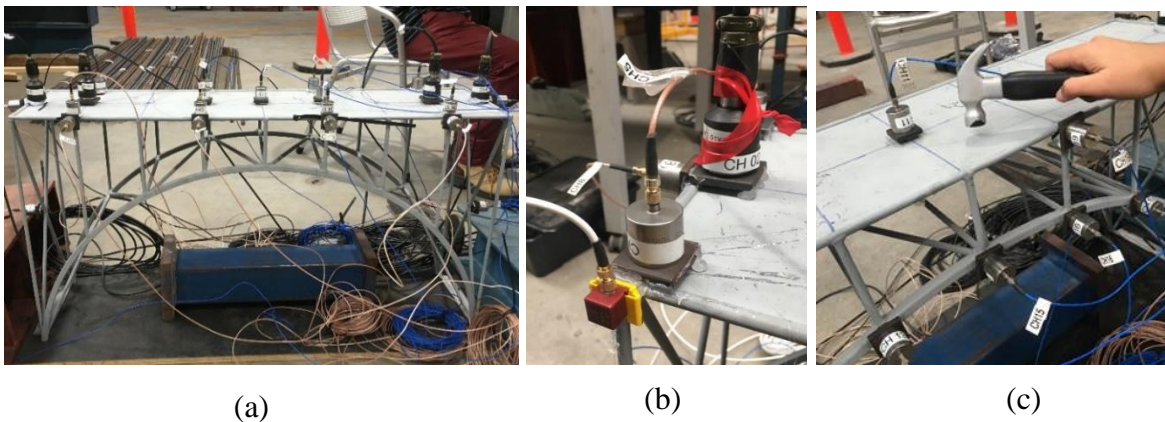
## Validation of proposed method and modelling techniques

### Experimental testing

Before the application of the developed method for damage detection, a comprehensive laboratory test was conducted on a small scale deck type steel arch bridge structure in order to validate the proposed method and the finite element modelling techniques.

The test model had a span of 1m and a height of 0.4 m. The deck had a width of 0.25m and was made from 2 mm thick steel plate, supported by 9, 6 mm diameter vertical struts at the edges as shown in Figure 3. All members of the bridge were made of general steel with Young's Modulus, density and Poisson ratio of  $2.05 \times 10^{11}$  Pa,  $7870 \text{ kgm}^{-3}$  and 0.3 respectively. The bridge was fixed to a plate at the base to represent fixed-fixed boundary conditions.

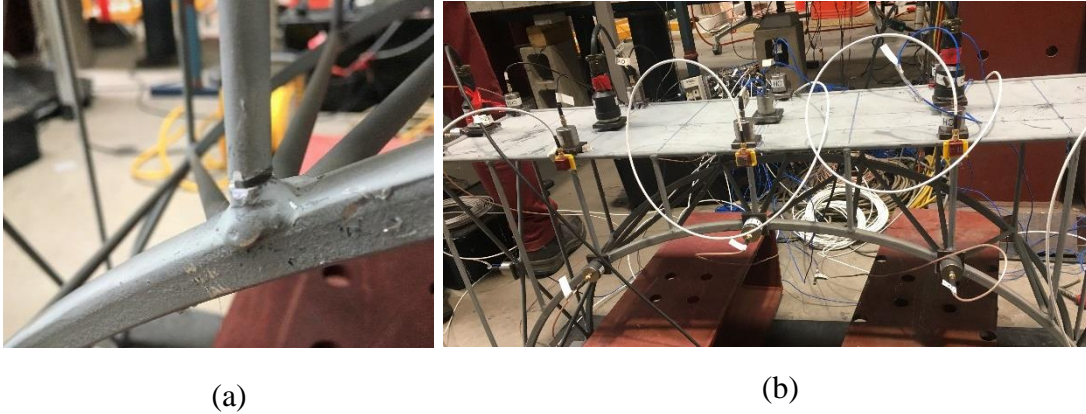
Free vibration testing was performed on the bridge model (Figure 3a) to obtain the vibration parameters of mode shapes and natural frequencies to validate the proposed damage detection method as well as the Finite Element (FE) model. In order to measure lateral and vertical accelerations the data acquisition system contained a total of 20 single-axial PCB® 393B05 integrated circuit piezoelectric accelerometers which can be self-calibrated within a few seconds and automatically pick up the precise acceleration at the position. Accelerometers were attached to selected nodes in the bridge as shown in Figure 3 and each of these will indicate the acceleration in the direction of its axis.



**Figure 3: Accelerometer arrangement and dynamic test on the bridge**

The acceleration data was acquired by a centralized National Instruments (NI) data acquisition system including NI cDAQ 9172 chassis, NI 9234 dynamic signal acquisition modules and an in-house LabVIEW-based data acquisition program to enable precise hardware-based synchronization<sup>31</sup>. Since the laboratory model cannot be excited naturally, random hammer tapping was conducted at many different locations/directions to simulate traffic and wind excitation on the bridge. (Figure 3c).

Data was acquired for a predetermined uninterrupted duration of 1.5 minutes so that the continuous signal length can be 1000-2000 times of the fundamental period of the bridge (approximate 0.005 second) to enable proper output-only modal analysis<sup>32</sup>. Few repeat tests were performed to eliminate any random errors and to improve the accuracy of results. The acceleration data was captured in the time domain and was conveyed to the ARTeMIS modal analysis software to retrieve modal parameters. The natural frequencies and mode shapes were determined by the Data Driven Stochastic Subspace Identification (SSI-DATA) in ARTeMIS modal analysis software<sup>33</sup>.



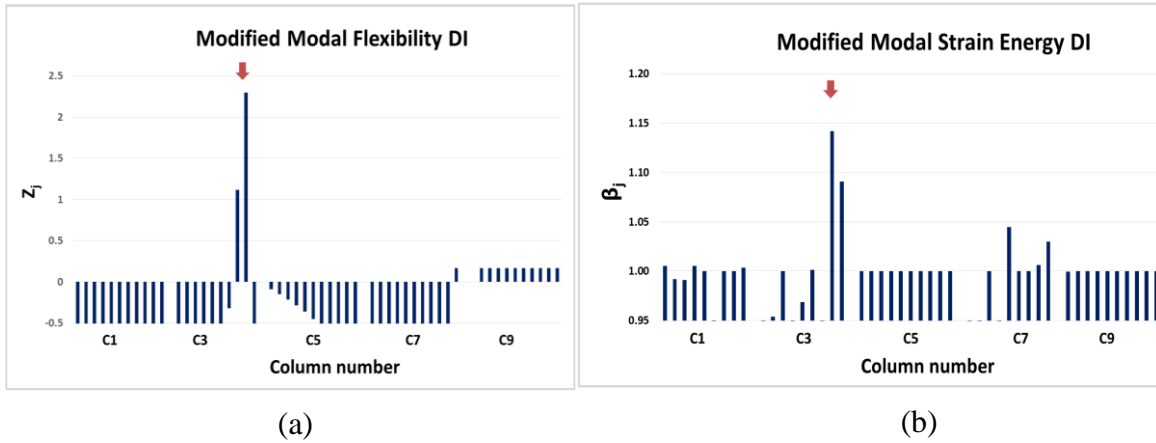
**Figure 4:** Column Damage on experimental model (a) damage location (b) accelerometer configuration

The free vibration test on the undamaged structure was considered as the baseline dynamic test which was followed by a dynamic test performed on the damaged structure. Physical damage was induced on the structure by removing some material from the 3<sup>rd</sup> vertical column and decreasing its connectivity with the rib, as shown in Figure 4 (a). The natural frequencies and mode shapes obtained from the structure in its healthy and damaged states will be used to validate the proposed method in the next section and the modelling techniques in the subsequent section.

### Experimental validation of the proposed method

Experimental validation of the developed method was carried out using the results from the experimental testing of the arch bridge model (as described above). Measured mode shapes and natural frequencies from the experimental free vibration testing of both the damaged and undamaged structure, using a limited number of sensors and in a typical laboratory environment (which invariably has noise pollution) are used to calculate the four component specific damage indices and then select the better performing DIs using the procedure outlined through [Eqs. 19, 20](#) and [21](#). These preferred DIs are then used to obtain the damage detection results and thereby verify the proposed method experimentally. Accelerometers were attached to the ends of each alternate column (Figure 4b) and cubic spline interpolation was used, where necessary, to enhance the mode shape data.

It is evident that the damage at the base of the 3rd vertical column (C3) of the bridge (Figure 4a) is correctly detected through the method developed in this paper by the two preferred component- specific (MF and MSE based) DIs as shown in the plots in Figure 5. The peaks of both modified damage indices clearly and correctly indicate the location of damage. As mentioned earlier, use of either one of the modified DIs would have sufficed, but results from both are recommended as they complement and supplement each other and provide adequate confidence in the predictions.

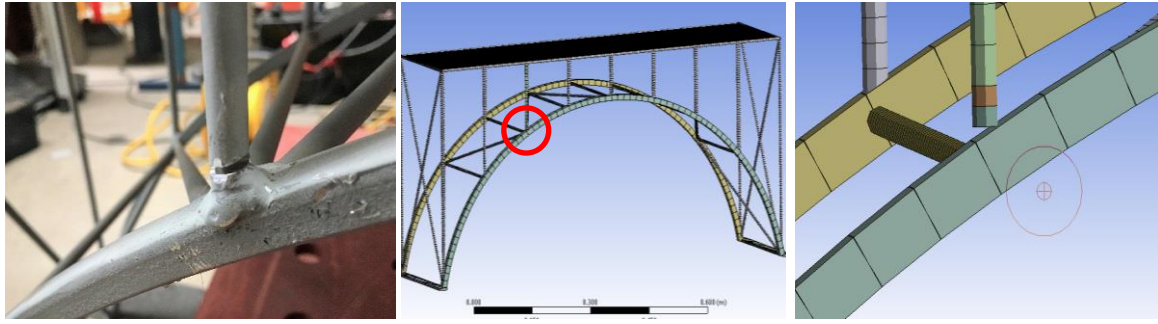


**Figure 5:** Predicting 3<sup>rd</sup> column (C3) damage by (a) Modified MF DI and (b) Modified MSE DI

## Validation of modelling techniques

The modelling techniques are next validated by comparing the results from free vibration analysis of the finite element model of the bridge with those from the experimental testing of the physical bridge (as described above) in both its healthy and damaged states.

The exact finite element model of the laboratory bridge model was created in ANSYS Workbench finite element software which is a commercially available FEM software, capable of developing complex structures with multibody parts and complex analyses. The geometry of the laboratory bridge was modelled at ANSYS Workbench DesignModeler as a 3D FE model. Each part (deck, vertical struts, arch rib, and wind bracings) was connected to the other by using the joint feature in Mechanical module of ANSYS workbench. General mild steel properties, mentioned above were assigned to each element of the structure. All elements, except the deck elements, were modelled with beam elements (BEAM 188) and the deck was modelled with shell elements (SHELL 181). Additional point masses were added to the model to account the masses of accelerometers. Damage was simulated in the FE model to match the physical damage in the bridge structure as shown in Figure 6. Prestressed Modal Analysis was conducted (incorporating the initial stress state of the structure under its self-weight) to obtain natural frequencies and mode shapes of the numerical model of the arch bridge<sup>34</sup>.



(a)

(b)

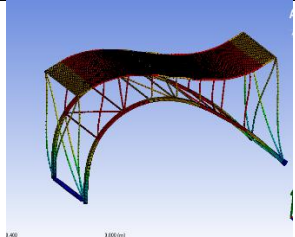
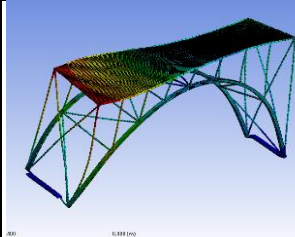
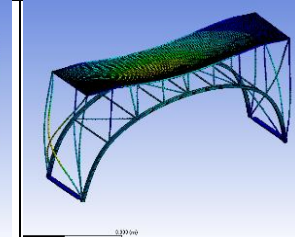
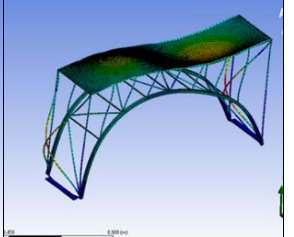
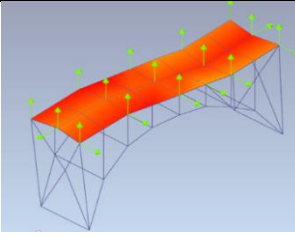
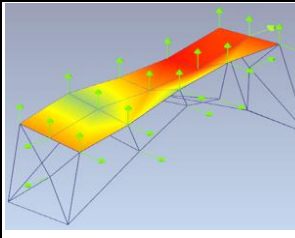
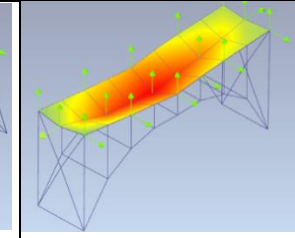
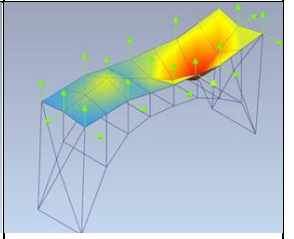
**Figure 6:** Column damage on (a) Experimental model (b) Numerical model

Model updating was performed to tune the structural parameters of the FE model to match with the experimental model. This was conducted manually by slightly adjusting the material properties, boundary condition, the fixity between deck plate, frame and other structural components. The masses of the accelerometers were added at the appropriate location in the FE model. Natural frequencies of the first four modes obtained from the FE model in its healthy and damaged states are compared with those from the experiments in Table 2, while the experimental and numerical mode shapes of the bridge model in its healthy state are shown in Table 3.

**Table 2:** Comparison of natural frequencies from experiments and numerical models under healthy and damaged states of the structure

Mode	Undamaged state			Damaged state		
	Natural Frequencies (Hz)		$f_{\text{error}}$ (%)	Natural Frequencies (Hz)		$f_{\text{error}}$ (%)
	$f_{\text{exp}}$	$f_{\text{FEM}}$		$f_{\text{exp}}$	$f_{\text{fem}}$	
1	20.00	21.18	5.50	19.00	19.80	4.20
2	33.00	33.36	1.09	33.00	31.85	-3.40
3	54.25	53.54	-1.30	53.00	50.40	-4.50
4	64.25	61.95	-3.40	64.00	62.00	-0.15

**Table 3:** Numerical (top) and experimental (bottom) mode shapes of the laboratory scale arch bridge structure

Mode 1	Mode 2	Mode 3	Mode 4
			
21.18 Hz	33.36 Hz	53.54 Hz	61.95 Hz
			
20.00 Hz	33.00 Hz	54.25 Hz	64.25 Hz

It can be seen that the results from the analysis of the finite element model of the laboratory bridge compare reasonably well with the experimental results and provide confidence in the modelling techniques. These modelling techniques are then used to model the full scale bridge that will be used in further damage detection studies.

### Damage detection in full scale two hinged arch bridge

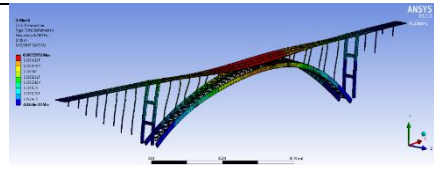
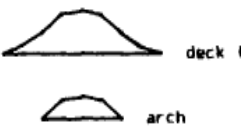

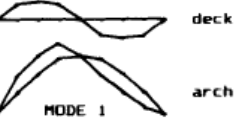
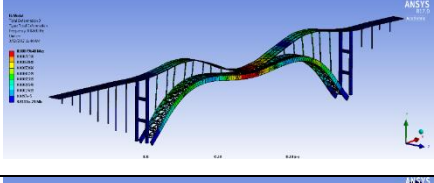
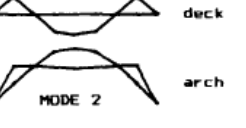
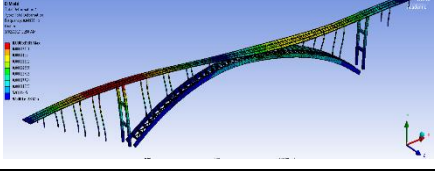
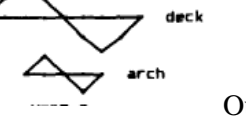
To illustrate the applicability of the proposed damage detection technique to a full scale long span arch bridge, a complete finite element model of Cold Spring Canyon Bridge is developed using ANSYS finite element modelling software. Cold Spring Canyon Bridge is a long-span, deck type steel arch bridge with a span of 213 m and a rise of 36.27 m. The main ribs are restrained except for the rotational degrees-of-freedom about the transverse axis at the abutments, thus creating a two hinged arched mechanism. The deck is supported over the arch by vertical columns which are hinged at the panel points and at the end of towers above the arch abutments. The deck slab which connects to the continuing road is restrained longitudinally at one end of the approach span. There were no additional expansion joints present over the arch span<sup>35</sup> (Figure 7).



**Figure 7: Cold Spring Canyon Bridge**

The geometry of the Cold Spring Canyon Bridge was developed using Workbench of ANSYS finite element software. The bridge was modelled as a 3D FE model with several parts (deck, arch ribs, cross bracings, columns etc.) which were ultimately connected via relevant connectivity (joint feature) in the Mechanical module. The global mode shapes of the bridge obtained from the present FE model were compared with those from the 2D analysis Dusseau & Wen<sup>35</sup>, and reasonably good agreement between the two sets of mode shapes was obtained, as shown in Table 4.

**Table 4: Comparison of mode shapes of Cold Spring Canyon Bridge**


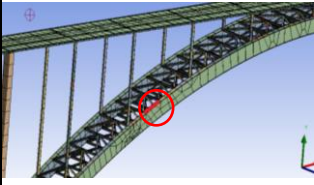
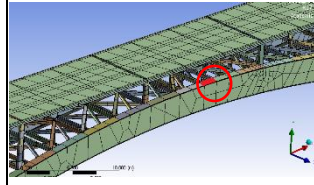
Mode	Freq.	Present Results	Results from 2D Analysis of Dusseau and Wen (1989)
1st Mode	0.4564 Hz		 deck 1 arch In-plane
2nd Mode	0.4725 Hz		 deck MODE 1 arch In-plane
3rd Mode	0.826 Hz		 deck MODE 2 arch In-plane
4th Mode	0.849 Hz		 deck arch Out-of-plane



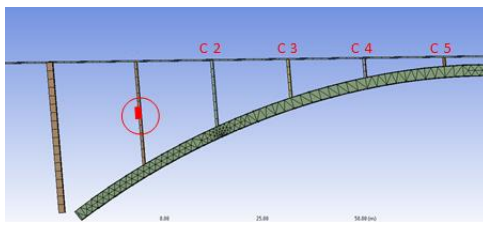
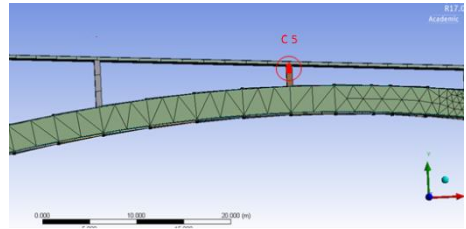
## Results and Discussion

### Single damage scenarios without noise

**Table 5: Damage Scenarios of arch rib**

Damage Scenario			
	Rib Damage Case 1	Rib Damage Case 2	Rib Damage Case 3
Damaged Element	Damage at arch spring	Damage at 1/4 span of rib	Damage at crown
Stiffness Reduction	10%	10%	10%

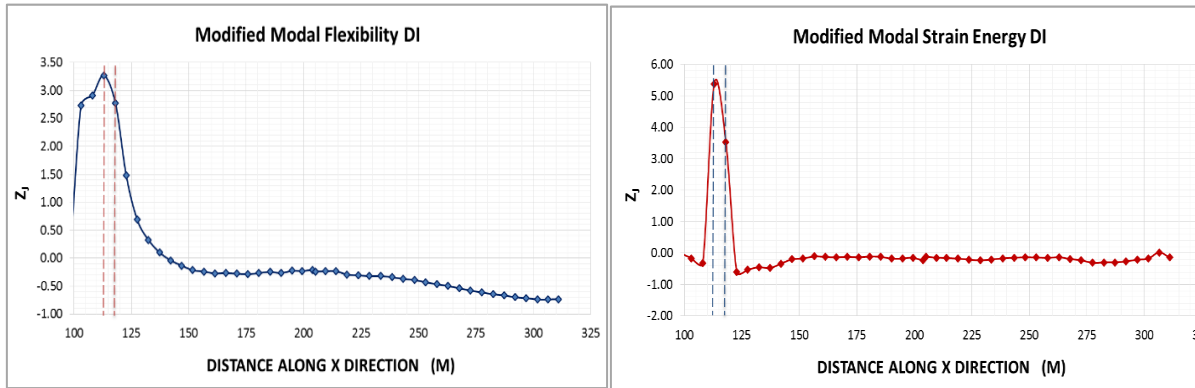
**Table 6: Damage Scenarios of vertical columns**

Damage Scenario		
	Vertical column damage Case 1	Vertical column damage Case 2
Damaged Element	Damage at mid of the long column	Damage at the edge of the short column
Stiffness Reduction	10%	10%

The versatility of the proposed dual criteria method for damage detection in a long span arch bridge is demonstrated by its application to a range of different damage cases in the Cold Spring Canyon Bridge. Damage was inflicted at three different locations on the arch rib and on two different vertical columns of this bridge as illustrated in Table 5 and Table 6. Damage was induced as a stiffness reduction by reducing the Young's Modulus by 10%. Modal parameters of natural frequencies and mode shapes of the healthy and each damaged structure were extracted from FE modal analyses. The proposed modified modal flexibility and strain energy based damage indices described in section 2 are calculated separately for

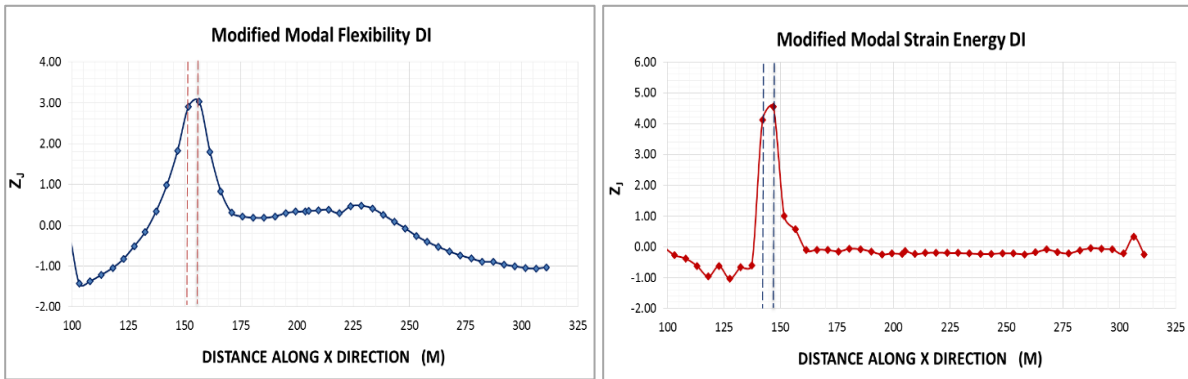
each damage case using the first four global modes of vibration and are plotted along the bridge. The peaks in the plots of these damage indices are expected to indicate the location of the damage and plots are shown in Figure 8 – Figure 12 for above five different damage cases.

- Rib Damage Case 1: Damage at arch spring



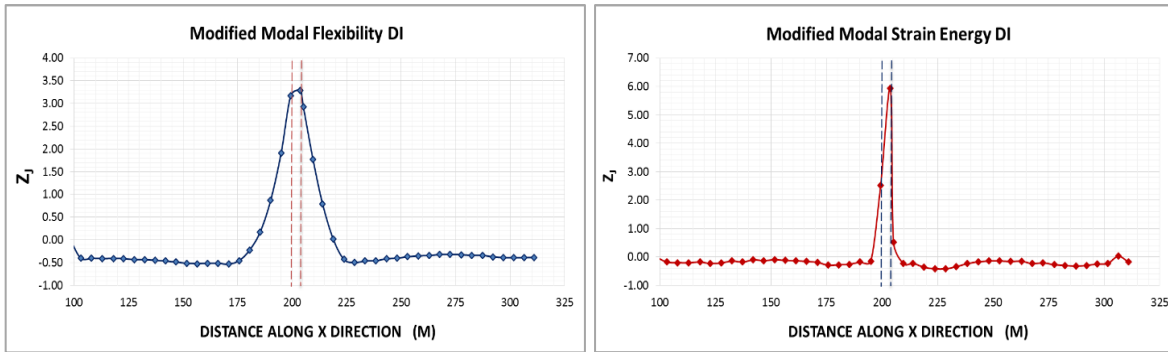
**Figure 8:** Plots of Modified MF and Modified MSE DIs for rib damage case 1

- Rib Damage Case 2: Damage at quarter span of the arch rib



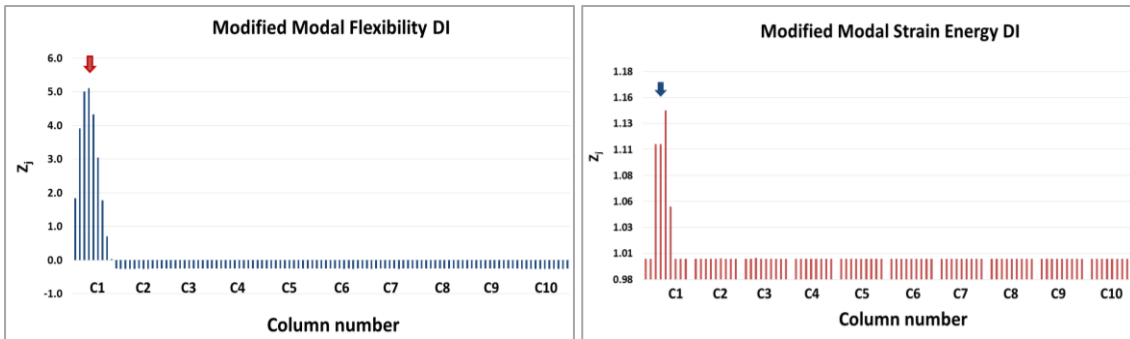
**Figure 9:** Plots of Modified MF and Modified MSE DIs for rib damage case 2

- Rib Damage Case 3: Damage at mid span of the arch rib



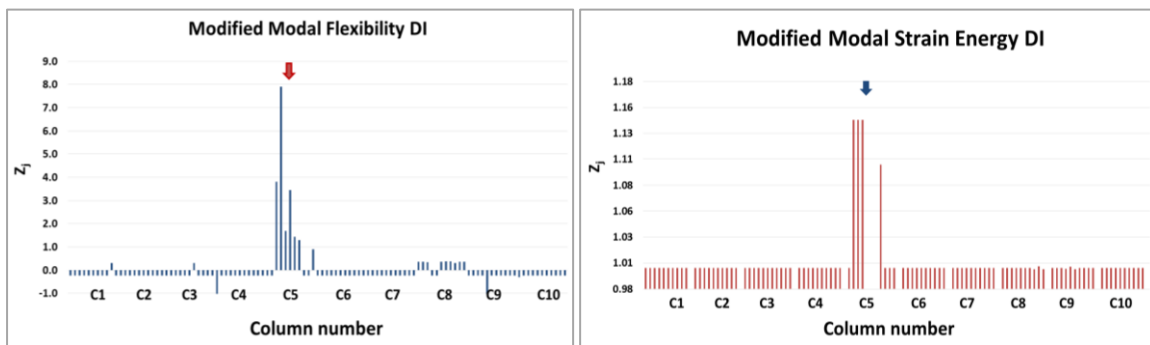
**Figure 10:** Plots of Modified MF and Modified MSE DIs for rib damage case 3

- Vertical Column Damage Case 1:



**Figure 11:** Plots of MMF and MMF DI for damage at middle of long column C1

- Vertical Column Damage Case 2:



**Figure 12:** Plots of MMF and MMF DI for damage at the edge of short column C5

It is clear from the above Figures that both proposed damage indices are capable of detecting damage in the arch rib and vertical columns without any false alarms. Though

either one of these modified DI would be effective for damage detection, this paper recommends the simultaneous use of both DIs to cross check and obtain unambiguous results.

### Multiple damage scenarios and effect of noise

In the practical context, vibration responses of the structures are allied with uncertainties in modal frequencies and mode shape data, such as measurement noise and computational errors. Thus it is important to check the accuracy of the proposed method in the presence of noise in the modal data. Since the vibration responses generated through the finite element model are free from noise, the noise contaminated mode shape data is created using [Eq. 22](#) by Shi et al. <sup>8</sup>.

$$\overline{\phi}_{xi} = \phi_{xi}(1 + \gamma_x^\phi \rho_x^\phi |\phi_{max,i}|) \quad (22)$$

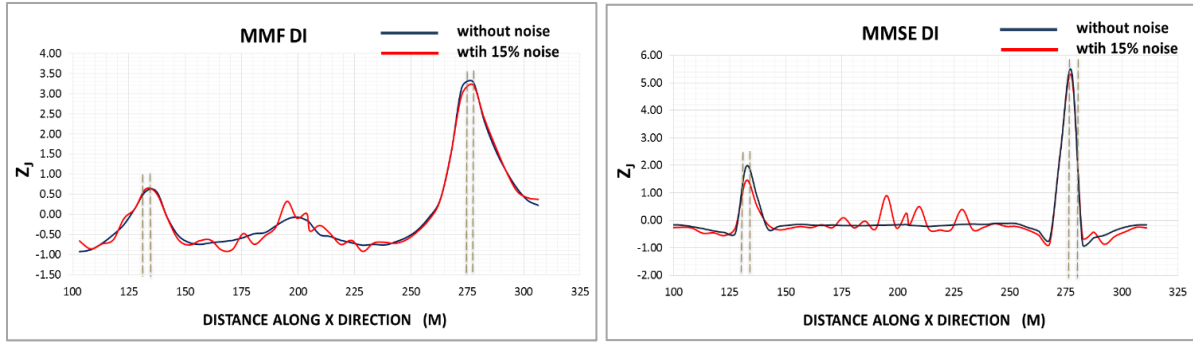
The terms  $\overline{\phi}_{xi}$  and  $\phi_{xi}$  are mode shape component of the  $i^{th}$  mode of vibration at location  $x$  with and without noise respectively.  $\rho_x^\phi$  denotes the random noise level and  $\gamma_x^\phi$  refers to a random number with mean equal to zero and variance equal to 1 and  $|\phi_{max,i}|$  is the absolute value of the largest component in the  $i^{th}$  mode shape.

Two multiple damage cases of the rib and one multiple column damage case (as illustrated in Table 7) are considered in this section with and without noise. Each case contains similar or different damage intensities. In addition, 5% ,10% and 15% random noise levels are introduced to mode shapes retrieved through the FE analysis. The two damage indices are calculated and plotted against the length along the rib and the column number and shown below in

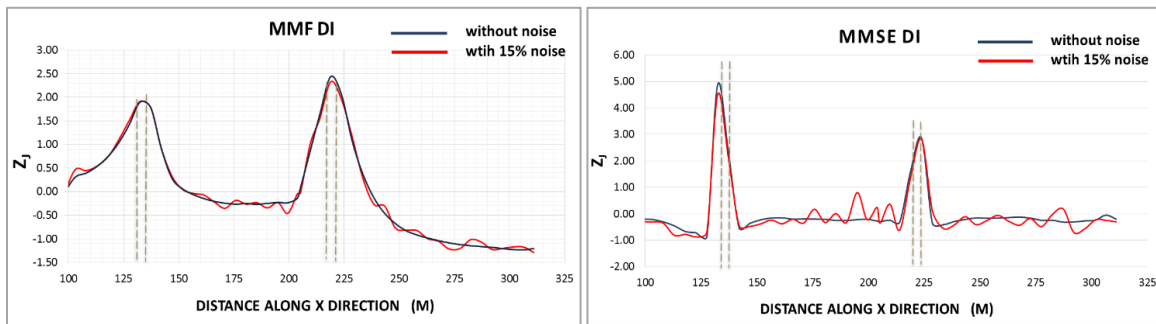
Figure 13- Figure 16. The peaks in the plots of these damage indices are expected to indicate the location of the damage.

**Table 7: Multiple Damage Scenarios of arch rib and columns with noise polluted data**

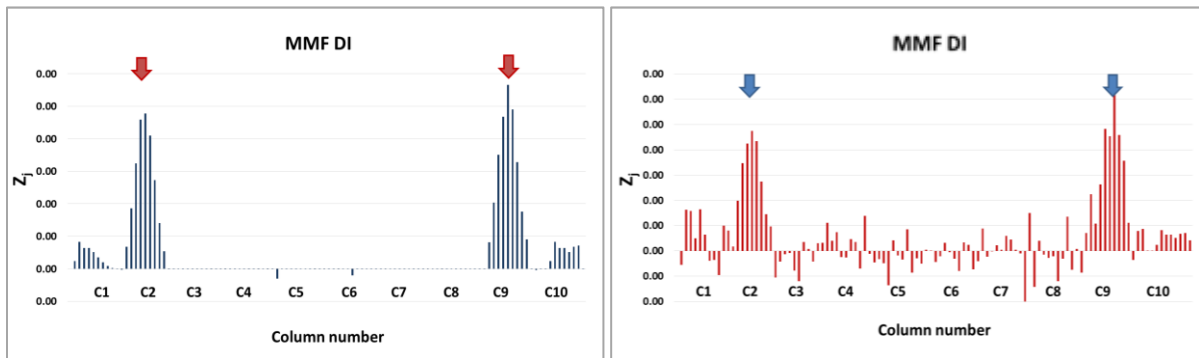
Damage case	Damage Location	Damage Intensity	Noise level
Multiple Damage Case 1	Damage at the rib location $x = 132.4\text{m}$ and $x = 223.8\text{m}$	10% stiffness reduction at both locations	15%
Multiple Damage Case 2	Damage at the rib location $x = 132.4\text{m}$ and $x = 277.5\text{m}$	5% and 10% stiffness reductions respectively	15%
Multiple Damage Case 3	Damage at the mid of 2 <sup>nd</sup> column and 9 <sup>th</sup> column	10% stiffness reduction at both columns	10%



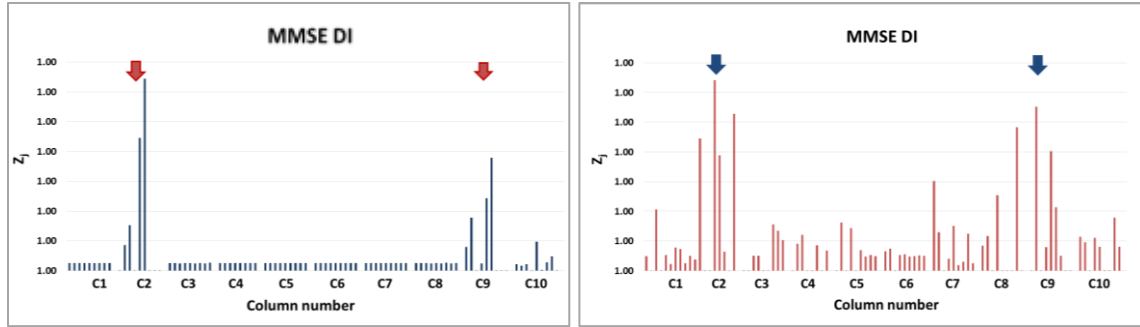
**Figure 13:** Plots of Modified DIs for damage case 1 with and without (15%) noise (a) Modified MF DI (b) Modified MSE DI



**Figure 14:** Plots of Modified DIs with and without 15% noise: (a) Modified MF DI (b) Modified MSE DI



**Figure 15:** Plots of Modified MF DIs with 10% damage at 2nd and 9th columns (a) without noise (b) with 10% noise

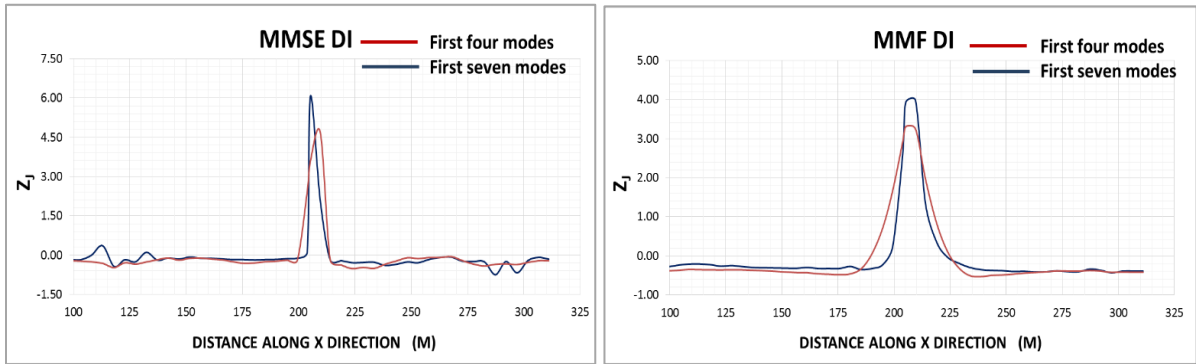


**Figure 16:** Plots of Modified MSE DIs with 10% damage at 2nd and 9th columns (a) without noise (b) with 10% noise

It is clearly evident from these Figures that the proposed modified DIs are capable of detecting and locating multiple damages in the arch bridge components with reasonable accuracy, even in the presence of 15% noise. Further, some traditional DIs are noise sensitive and can exhibit false alarms. In such situations the proposed dual criterial approach provides the benefit of complementing and supplementing the results to provide more accurate predictions of damage location.

### Influence of higher order modes in damage detection

The analyses above utilize the first four global modes of vibration to calculate the damage indices. In order to check the effect of including higher order modes, the damage indices were calculated using first seven global modes of vibration. The results of the two scenarios are illustrated in Figure 17. A damage of 10% stiffness reduction was applied at the mid span of the rib and the MMF and MMSE damage indices were calculated and plotted using (i) first four and (ii) first seven modes of vibration. The results show that the first four modes are adequate to detect and locate the damage in the arch rib and the use of more higher order modes will therefore not contribute much towards improving the damage detection. In practice it is difficult to obtain many accurate higher order global modes of vibration of the bridge and hence the method proposed in this paper is beneficial as it can detect and locate the damage by using a few initial modes of vibration.



**Figure 17:** Plots of Modified MSE and MF DIs with first four and first seven global modes of vibration

## Conclusion

Variation in vibration characteristics of a structure are used to develop and present a dual criteria approach that can accurately detect and locate damage in the structural components of deck type arch bridges. In this approach the traditional MF and MSE based indices are modified by decomposing each of them into vertical and lateral indices, extracting the larger values of each type and normalizing them to capture the damage location very effectively. The proposed method and the modelling techniques are experimentally validated through the testing of a laboratory arch bridge model. The feasibility of the proposed procedure is illustrated via its application to detect damage in the major structural components of arch bridges. A range of damage scenarios is considered in the laboratory bridge model and a (full scale) long span arch bridge involving damage in the arch rib as well as in the vertical columns. Results demonstrate the capability of the proposed method to detect single as well as multiple damages even in the presence of noise polluted data. Though both DIs performed reasonably well in all the damage scenarios treated in this paper, this might not be the case in some of the other damage scenarios. The dual-criteria approach will be very effective in those cases as the results obtained from either DI will complement and supplement the results from the other DI and lead to more reliable prediction of the damage location. Reliable prediction of the damage location through the use of the proposed dual criteria approach will prevent unsafe decisions or unnecessary examinations of false alarms. Further, the use of higher modes of vibration for detecting damage in the structural components was investigated. The results show that for accurate detection of damage, the first four global modes of vibration are sufficient and there are no added benefits by using larger number of mode shapes which are practically difficult to obtain. Finally the procedure developed in this research can be extended to detect and locate damage in other types of arch bridges and will contribute towards the safe and efficient performance of these types of bridge structures across Australia and elsewhere.

## Acknowledgement

This research forms a part of a continuing study of structural health monitoring of structures conducted at the Queensland University of Technology (QUT), Australia. The first author gratefully acknowledge the guidance provided by the supervisors, facilities and support for experiments provided by QUT pilot plant at Banyo and the QUT Postgraduate Research Scholarship

## References

1. Australia Standards: AS 5100.7-Bridge Design. Bridge Assessment, 2017, Standards, Australia, Sydney, NSW, Australia.
2. Chan TH, Wong K, Li Z, et al. Structural health monitoring for long span bridges: Hong Kong experience and continuing onto Australia. In: Chan TH and Thambiratnam DP (eds) *Structural Health Monitoring in Australia*. New York: Nova Science Publishers, Inc., 2011, pp.1-32.
3. Rizos P, Aspragathos N and Dimarogonas A. Identification of crack location and magnitude in a cantilever beam from the vibration modes. *Journal of sound and vibration* 1990; 138: 381-388.
4. Hong JC, Kim Y, Lee H, et al. Damage detection using the Lipschitz exponent estimated by the wavelet transform: applications to vibration modes of a beam. *International journal of solids and structures* 2002; 39: 1803-1816.
5. Shih HW, Thambiratnam DP and Chan THT. Vibration based structural damage detection in flexural members using multi-criteria approach. *Journal of Sound and Vibration* 2009; 323: 645-661. DOI: <http://dx.doi.org/10.1016/j.jsv.2009.01.019>.
6. Cornwell P, Doebling SW and Farrar CR. Application of the strain energy damage detection method to plate-like structures. *Journal of sound and vibration* 1999; 224: 359-374.
7. Contursi T, Messina A and Williams E. A multiple-damage location assurance criterion based on natural frequency changes. *Journal of vibration and control* 1998; 4: 619-633.
8. Shi Z, Law S and Zhang L. Damage localization by directly using incomplete mode shapes. *Journal of Engineering Mechanics-ASCE* 2000; 126: 656-660.
9. Law S, Shi Z and Zhang L. Structural damage detection from incomplete and noisy modal test data. *Journal of Engineering Mechanics* 1998; 124: 1280-1288.
10. Wang S, Zhang J, Liu J, et al. Comparative study of modal strain energy based damage localization methods for three-dimensional structure. In: *The Twentieth International Offshore and Polar Engineering Conference* 2010, International Society of Offshore and Polar Engineers.
11. Li H, Yang H and Hu SLJ. Modal strain energy decomposition method for damage localization in 3D frame structures. *Journal of engineering mechanics* 2006; 132: 941-951.
12. Shih HW, Thambiratnam D and Chan TH. Damage detection in truss bridges using vibration based multi-criteria approach. *Structural Engineering and Mechanics* 2011; 39: 187.
13. Wang FL, Chan TH, Thambiratnam DP, et al. Correlation-based damage detection for complicated truss bridges using multi-layer genetic algorithm. *Advances in Structural engineering* 2012; 15: 693-706.
14. Shih H, Thambiratnam D and Chan T. Damage detection in slab-on-girder bridges using vibration characteristics. *Structural Control and Health Monitoring* 2013; 20: 1271-1290.
15. Wickramasinghe WR, Thambiratnam DP, Chan TH, et al. Vibration characteristics and damage detection in a suspension bridge. *Journal of Sound and Vibration* 2016; 375: 254-274.
16. Jia S and Dhanasekar M. Detection of rail wheel flats using wavelet approaches. *Structural Health Monitoring* 2007; 6: 121-131.



17. Doebling SW, Farrar, C.R., Prime, M.B. and Shevitz, D.W., . *Damage identification and health monitoring of structural and mechanical systems from changes in their vibration characteristics: a literature review*. Los Alamos National Lab., NM (United States). 1996.
18. Salehi M, Rad SZ, Ghayour M, et al. A non model-based damage detection technique using dynamically measured flexibility matrix. *Iranian Journal of Science and Technology Transactions of Mechanical Engineering* 2011; 35: 1.
19. Fan W and Qiao P. Vibration-based damage identification methods: a review and comparative study. *Structural Health Monitoring* 2011; 10: 83-111.
20. Allemang RJ. The modal assurance criterion—twenty years of use and abuse. *Sound and vibration* 2003; 37.
21. Lieven N and Ewins D. Spatial correlation of mode shapes, the coordinate modal assurance criterion (COMAC). In: *Proceedings of the sixth international modal analysis conference* 1988, pp.690-695.
22. Pandey AK and Biswas M. Damage Detection in Structures Using Changes in Flexibility. *Journal of Sound and Vibration* 1994; 169: 3-17. DOI: <http://dx.doi.org/10.1006/jsvi.1994.1002>.
23. Pandey AK and Biswas M. Experimental verification of flexibility difference method for locating damage in structures. *Journal of Sound and Vibration* 1995; 184: 311-328. DOI: <http://dx.doi.org/10.1006/jsvi.1995.0319>.
24. Praveen Moragasipitiya HN, Thambiratnam DP, Perera NJ, et al. Development of a vibration based method to update axial shortening of vertical load bearing elements in reinforced concrete buildings. *Engineering Structures* 2013; 46: 49-61. DOI: <http://dx.doi.org/10.1016/j.engstruct.2012.07.010>.
25. Shih HW, Thambiratnam DP and Chan TH. Vibration based structural damage detection in flexural members using multi-criteria approach. *Journal of sound and vibration* 2009; 323: 645-661.
26. Toksoy T and Aktan A. Bridge-condition assessment by modal flexibility. *Experimental Mechanics* 1994; 34: 271-278.
27. Farrar CR and Jauregui DA. Comparative study of damage identification algorithms applied to a bridge: I. Experiment. *Smart materials and structures* 1998; 7: 704.
28. Stubbs N, Kim JT and Farrar C. Field verification of a nondestructive damage localization and severity estimation algorithm. In: *Proceedings-SPIE the international society for optical engineering* 1995, pp.210-210. SPIE INTERNATIONAL SOCIETY FOR OPTICAL.
29. Choi F, Li J, Samali B, et al. Application of the modified damage index method to timber beams. *Engineering structures* 2008; 30: 1124-1145.
30. Stubbs N and Garcia G. Application of pattern recognition to damage localization. *Computer-Aided Civil and Infrastructure Engineering* 1996; 11: 395-409.
31. Nguyen A, Chan TH, Thambiratnam DP. Output-only modal testing and monitoring of civil engineering structures: Instrumentation and test management. *International Conference on Structural Health Monitoring of Intelligent Infrastructure (SHMII-08)*. Brisbane, Australia2017, p. 1-12.
32. Nguyen T, Chan TH, Thambiratnam DP, et al. Development of a cost-effective and flexible vibration DAQ system for long-term continuous structural health monitoring. *Mechanical Systems and Signal Processing* 2015; 64: 313-324.
33. Nguyen T, Chan TH and Thambiratnam DP. Effects of wireless sensor network uncertainties on output-only modal analysis employing merged data of multiple tests. *Advances in Structural Engineering* 2014; 17: 319-329.
34. ANSYS®. Academic Research, Release 18, Help System, Coupled Field Analysis Guide. *ANSYS, Inc.*
35. Dousseau RA and Wen RK. Seismic responses of deck-type arch bridges. *Earthquake engineering & structural dynamics* 1989; 18: 701-715.